

# Raman analysis of perrhenate and pertechnetate in alkali salts and borosilicate glasses

Paul L. Gassman,<sup>a\*</sup> John S. McCloy,<sup>b</sup> Chuck Z. Soderquist<sup>a</sup> and Michael J. Schweiger<sup>a</sup>



Sodium borosilicate glasses containing rhenium or technetium were fabricated and their vibrational spectra studied using confocal Raman microscopy. Glass spectra were interpreted relative to new high-resolution spectra of pure crystalline  $\text{NaReO}_4$ ,  $\text{KReO}_4$ ,  $\text{NaTcO}_4$ , and  $\text{KTcO}_4$  salts. Spectra of perrhenate and pertechnetate glasses exhibited sharp Raman bands, characteristic of crystalline salt species, superimposed on spectral features of the borosilicate matrix. At low concentrations of added  $\text{KReO}_4$  or  $\text{KTcO}_4$ , the characteristic pertechnetate and perrhenate features are weak, whereas at high additions, sharp peaks from crystal field-splitting and  $C_{4h}$  symmetry dominate glass spectra, clearly indicating  $\text{ReO}_4^-$  or  $\text{TcO}_4^-$  is locally coordinated with K and/or Na. Peaks indicative of both K and Na salts are evident in many Raman spectra, with the Na form being favored at high concentrations of the source chemicals, where more  $\text{K}^+$  is available for ion exchange with  $\text{Na}^+$  from the base glass. The observed ion exchange likely occurred within depolymerized channels where nonbridging oxygens create segregation from the glass network in regions containing anions such as  $\text{ReO}_4^-$  and  $\text{TcO}_4^-$  as well as excess alkali cations. Although this anion exchange provides evidence of chemical mixing in the glass, it does not prove the added salts were homogeneously incorporated in the glass. The susceptibility to ion exchange from the base glass indicates that long-term immobilization of Tc in borosilicate glass must account for excess charge compensating alkali cations in melt glass formulations. Published 2014. This article is a U. S. Government work and is in the public domain in the USA.

Additional supporting information may be found in the online version of this article at the publisher's web site.

**Keywords:** perrhenate; pertechnetate; borosilicate; confocal Raman; technetium

## Introduction

A priority goal of the US Department of Energy (US DOE) is to dispose of nuclear wastes accumulated in large underground tanks at the Hanford Nuclear Reservation in eastern WA, USA.<sup>[1]</sup> These nuclear wastes date from the Manhattan Project of World War II and from plutonium production during the Cold War. The DOE plans to separate highly radioactive wastes from low activity wastes (LAWs) and to isolate high-activity wastes in vitrified forms (glass) for long-term disposal. Included in the inventory of highly radioactive wastes is large volumes of  $^{99}\text{Tc}$  ( $\sim 9 \times 10^2$  TBq or  $\sim 2.5 \times 10^4$  Ci or  $\sim 1500$  kg).<sup>[2]</sup>

This paper describes the coordinated environment of perrhenates and pertechnetates (1) in glasses when  $\text{KReO}_4$  or  $\text{KTcO}_4$  were added to the simulated LAW<sup>[3,4]</sup> glass and (2) in crystalline compounds. The  $\text{KReO}_4$  or  $\text{KTcO}_4$  was added to the glass in order to study the impact of  $^{99}\text{Tc}$  on the properties and performance of highly radioactive glass formulations for long-term storage. Raman microscopy was used here to probe local environments in the glass structure and to study the crystallization behavior previously observed on the surface of the LAW glass.<sup>[3,4]</sup> The pertechnetate ion ( $\text{TcO}_4^-$ ) is the dominant form of Tc metal in the oxidizing environment of the waste tanks. Preliminarily, perrhenate ( $\text{ReO}_4^-$ ) was used as a nonradioactive surrogate for pertechnetate to probe the effects of the ion on the coordinated silicate, borate, and aluminate networks. Later,  $^{99}\text{TcO}_4^-$  was used for direct measurement of its structural and chemical effects on the

borosilicate glass networks. It was expected that incorporation of Tc and Re in glasses would be somewhat different because of known differences in oxidation-reduction potential.<sup>[5,6]</sup>

The incorporation of  $\text{ReO}_4^-$  in aluminoborosilicate glasses was previously measured by conventional Raman spectroscopy, X-ray absorption near edge structure spectroscopy, nuclear magnetic resonance spectrometry, and X-ray diffraction (XRD) analysis.<sup>[4,7]</sup> A subset of these measurements were performed on analogous Tc-containing glasses, and results are presented elsewhere.<sup>[8]</sup>

This work presents data from high spatial-resolution and high spectral-resolution Raman microscopy, which probed the local structure within the glasses as well as crystalline phases on the bulk glasses. These measurements may guide glass formulations to provide better long-term durability of  $^{99}\text{Tc}$ -containing aluminoborosilicate glasses, specifically by providing insight into the local environment around pertechnetate species. As part of this effort, new high-resolution Raman spectra were obtained from pure alkali perrhenate and pertechnetate salts:  $\text{NaReO}_4$ ,  $\text{KReO}_4$ ,  $\text{NaTcO}_4$ , and  $\text{KTcO}_4$ . To our knowledge, the full Raman spectrum of  $\text{NaTcO}_4$  has

\* Correspondence to: Paul L. Gassman, Pacific Northwest National Laboratory, Richland, WA 99352, USA. E-mail: pl.gassman@pnl.gov

<sup>a</sup> Pacific Northwest National Laboratory, Richland, WA, 99352, USA

<sup>b</sup> School of Mechanical and Materials Engineering, Washington State University, Pullman, WA, 99164, USA

never been presented before (a partial spectrum was provided in 9), and no comparison of the spectra of these four compounds has been offered. Presented here are exemplar spectra and vibrational assignments of peaks from these model species and comparisons to peaks from alumino-borosilicate glasses containing  $\text{KReO}_4$  and  $\text{KTcO}_4$ . Raman spectra were analyzed for evidence of perturbations of the alumino-borosilicate networks after adding  $\text{KReO}_4$  or  $\text{KTcO}_4$  at varying concentrations to the LAW glass. The LAW glass has the following composition by weight: 6.1%  $\text{Al}_2\text{O}_3$ , 10%  $\text{B}_2\text{O}_3$ , 2.07%  $\text{CaO}$ , 0.02%  $\text{Cr}_2\text{O}_3$ , 5.5%  $\text{Fe}_2\text{O}_3$ , 0.47%  $\text{K}_2\text{O}$ , 1.48%  $\text{MgO}$ , 21%  $\text{Na}_2\text{O}$ , 45.3%  $\text{SiO}_2$ , 0.16%  $\text{SO}_3$ , 1.4%  $\text{TiO}_2$ , 3.5%  $\text{ZnO}$ , and 3%  $\text{ZrO}_2$ .

The coordinated environment of rhenium in solution and in crystalline salts has been a subject of study for many years. Beintema<sup>[10]</sup> and Fonteyne<sup>[11]</sup> proposed octahedral coordination for rhenium in solution, although Beintema found tetrahedral coordination in crystalline alkali perrhenates. Claassen and Zielen<sup>[12]</sup> measured the infrared and Raman spectra of dilute solutions of perrhenate and used the numerical methods of Heath and Linnett<sup>[13]</sup> to determine that perrhenate ( $\text{ReO}_4^-$ ) exists in tetrahedral coordination in both solutions and in crystalline solids. Since this time, a few authors have revisited the vibrations of perrhenate in solution<sup>[14–17]</sup> as well as in the alkali salts  $\text{KReO}_4$ <sup>[18–20]</sup> and  $\text{NaReO}_4$ <sup>[19,20]</sup>. Rhenium has remained of interest because of its use as a surface catalyst for a variety of organic syntheses.<sup>[21]</sup>

Similarly, technetium has remained of interest since its discovery because of its role in nuclear processes and concern over its long-term environmental disposal. Several studies have been made of the Raman spectra of pertechnetate ( $\text{TcO}_4^-$ ) in solution.<sup>[15,16,18,22–24]</sup> However, there have been few reports of the Raman spectrum of  $\text{KTcO}_4$ <sup>[17,18,25]</sup> and only one of  $\text{NaTcO}_4$ .<sup>[9]</sup> McKeown and coworkers<sup>[22]</sup> are the only ones to report Raman spectra of technetium in glass. They describe pertechnetate in glass as being similar to the free-ion vibration but shifted up to 20 wavenumbers because of the local presence of a particular alkali species.

## Experimental

Glasses containing varying concentrations of rhenium and technetium were prepared according to the methods of McCloy and coworkers<sup>[26]</sup> by melting glass frits of the composition above at 1000 °C for 2 h in sealed silica tubes with potassium salts of Re or Tc oxide. Target concentrations of rhenium in glass varied from 100 to 10 000 ppm Re by mass. The solubility of Re in glass was previously determined to be ~3000 ppm Re,<sup>[4]</sup> so samples at higher concentrations contained crystalline inclusions of Re salts in the bulk and/or on the surface.<sup>[3]</sup> Glasses examined here with Raman microscopy were those above the solubility limit of Re, namely, 4000 ppm Re, 6415 ppm Re, 6415 ppm Re (no sulfate<sup>[7]</sup>), and 10 000 ppm Re. Technetium concentrations in glasses varied from 500 to 6000 ppm Tc, with some glasses made under slightly reducing conditions. The solubility of Tc by mass was determined to be ~2000 ppm Tc for the LAW glass as prepared and ~3000 ppm Tc for the same glass under slightly reducing conditions.<sup>[8]</sup> Oxidation states of Tc and Re in the glasses were  $\text{Tc(VII)}$  (i.e.  $\text{TcO}_4^-$ ),  $\text{Tc(IV)}$ , and  $\text{Re(VII)}$  (i.e.  $\text{ReO}_4^-$ ).<sup>[4,8]</sup> Technetium glasses analyzed using confocal Raman microscopy included 1000, 2000, 3000, and 4000 ppm Tc from added  $\text{KTcO}_4$ .

Reagent-grade  $\text{NaReO}_4$  and  $\text{KReO}_4$  (Alfa Aesar) were obtained for standards.  $\text{NaTcO}_4$  and  $\text{KTcO}_4$  were obtained as follows, with detailed procedures described elsewhere.<sup>[8]</sup> Solid, crystalline  $\text{KTcO}_4$  was prepared from ammonium pertechnetate ( $\text{NH}_4\text{TcO}_4$ , obtained from Oak Ridge National Laboratory). The  $\text{NH}_4\text{TcO}_4$  was partially decomposed from its own beta radiation and so was recrystallized by dissolving in a solution of ammonium hydroxide and hydrogen peroxide and then heated to reoxidize the technetium to pertechnetate and to decompose the excess peroxide. The solution was evaporated to recrystallize phase pure  $\text{NH}_4\text{TcO}_4$  as colorless crystals, which were washed with dry ethanol to remove water, then dried. Freshly recrystallized, dry  $\text{NH}_4\text{TcO}_4$  was weighed then dissolved in water, and a carefully measured stoichiometric amount of  $\text{K}_2\text{CO}_3$  was added to the  $\text{NH}_4\text{TcO}_4$  solution. The combined solution was evaporated to a low volume to expel  $(\text{NH}_4)_2\text{CO}_3$  and cause crystalline potassium pertechnetate to form. The pertechnetate product was washed with ethanol to remove water and then dried. Subsamples of the potassium pertechnetate were assayed for total technetium by liquid scintillation and found to be pure  $\text{KTcO}_4$  within analytical uncertainty. The product was free-flowing, white crystalline powder, a little finer than table salt. Sodium pertechnetate was prepared from potassium pertechnetate by passing an aqueous solution of  $\text{KTcO}_4$  through a sodium form cation exchanger. The solution was evaporated to crystallize  $\text{NaTcO}_4$ . The crystalline product was dried to a free-flowing powder.

Glass samples and crystalline precursor chemicals were encapsulated in two-piece plastic membrane boxes for spectral measurements to prevent inadvertent dispersion of radioactive Tc. Raman spectra were collected through an optical-grade quartz window epoxied to one side of the membrane box, which covered a 19-mm circular opening cut by a lathe. Technetium-containing powders or glass fragments were funneled into the center of a small nylon washer epoxied to the inside surface of the quartz window. The washer formed a cavity for the sample which was then sealed by epoxying a second quartz window over the nylon washer. The two halves of the boxes were then fit together and sealed using tape.

Glasses and crystalline materials were analyzed using a Horiba high-resolution confocal inverted-stage microscopic Raman spectrometer (LabRam HR8000) with 600 grooves/mm diffraction gratings, using a Nikon Eclipse Ti microscope. Laser excitation at 532 nm was provided by a Quantum Laser MPC-3000, which delivered ~20 mW of power to samples with an approximate spot diameter of 1  $\mu\text{m}$  on the samples. Spectra were recorded using a Peltier-cooled Horiba Synapse charge-coupled device (CCD) detector with a 1024  $\times$  256 pixel array. The spectrometer was calibrated using the line positions of a Hg pen lamp, and the band position of an amorphous Si wafer was used for frequency verification. Spectral resolution of the system, as described, was 1.8  $\text{cm}^{-1}$ /pixel with a laser spot size of 1.1  $\mu\text{m}$ . The spectrometer was preliminarily centered at 1000  $\text{cm}^{-1}$  Raman shift from the 532 nm laser excitation, precluding measurement of some external (skeletal) modes. The spectrometer position was changed to 950  $\text{cm}^{-1}$  to capture these low wavenumber peaks, allowing data collection from 1750 to ~50  $\text{cm}^{-1}$ . The number of spectral acquisitions, count times, and the diameter of the confocal iris were varied to maximize the signal-to-noise ratio of spectra. Most glass spectra were acquired for 10 min for improved signal-to-noise ratios. Crystalline  $\text{ReO}_4^-$  and  $\text{TcO}_4^-$  salts only required 2–10 s of acquisition time to achieve very strong signal-to-noise ratios.

## Results and discussion

Raman analyses of crystalline  $\text{NaReO}_4$ ,  $\text{KReO}_4$ ,  $\text{NaTcO}_4$ , and  $\text{KTcO}_4$  provided reference spectra for comparing  $\text{ReO}_4^-$  and  $\text{TcO}_4^-$  containing glasses. These reference spectra shown in Figs 1 and 2 reveal stretching and bending modes of perrhenates and pertechnetates, as well as external or lattice vibrations of these Na and K salts. Spectra from the crystalline solids did not require any spectral manipulations to provide very strong and well-resolved Raman bands. Fundamental vibrations, listed in Table 1 and Table 2, are compared with published values of aqueous anions, alkali salts, and to the acquired Raman spectra of Re-containing and Tc-containing glasses. Spectra from glasses containing low concentrations of  $\text{KReO}_4$  and  $\text{KTcO}_4$  were baseline corrected ('rubberband' correction) to provide consistent spectral resolution and band positions. Derived spectra were obtained by spectrally subtracting baseline LAW glass spectra from spectra of  $\text{KReO}_4$  and  $\text{KTcO}_4$  containing glasses. Spectral subtractions were sometimes aided by adjusting spectral amplitudes using a multiplicative constant. A spectral artifact observed in several glass spectra at  $390\text{ cm}^{-1}$  was attributed to poor spectral filtering of a plasma line from the HeNe laser. A few glass spectra contain weak peaks, which have not been resolvable to Raman vibrations from Tc and Re. These bands have been included in the bottom of Tables 1 and 2 as unassigned vibrations.

### Crystalline phases

Alkali perrhenates,  $\text{KReO}_4$ <sup>[28]</sup> and  $\text{NaReO}_4$ <sup>[21]</sup> and alkali pertechnetates,  $\text{KTcO}_4$ <sup>[29]</sup> and  $\text{NaTcO}_4$ <sup>[30]</sup> are all tetragonal with space group  $I41/a$ , possessing the Scheelite structure ( $\text{CaWO}_4$ ). Group

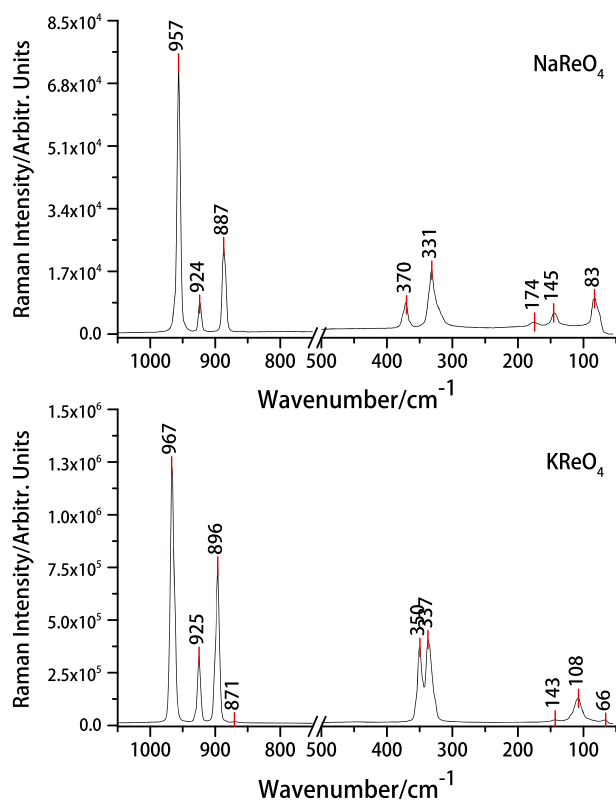


**Figure 1.** Raman spectra of pure crystalline  $\text{NaReO}_4$  (upper) and  $\text{KReO}_4$  (lower).

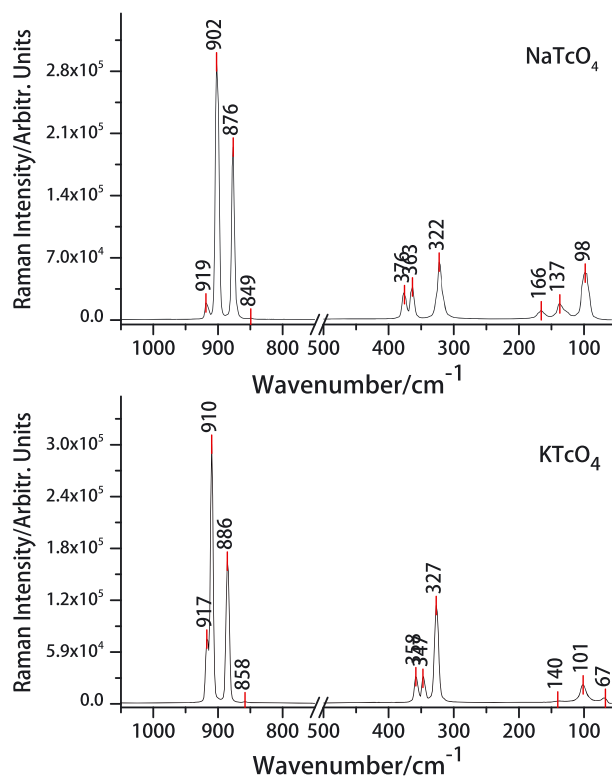


**Figure 2.** Raman spectra of pure crystalline  $\text{NaTcO}_4$  (upper) and  $\text{KTcO}_4$  (lower).

theory predicts that Re and Tc in K and Na salts has local symmetry  $C_{4h}$  from lattice symmetry of  $S_4$  from free-ion symmetry  $T_d$ .<sup>[17,19,20,31]</sup> A correlation diagram illustrating the mode derivations is shown in Fig. 3.

Comparing Raman spectra of crystalline  $\text{NaReO}_4$  and  $\text{KReO}_4$  shows the K salt exhibits higher symmetric ( $\nu_1$ ) and antisymmetric ( $\nu_3-E_g$ ) stretching modes. The symmetric ( $969\text{ cm}^{-1}$ ) and the antisymmetric stretch ( $898\text{ cm}^{-1}$ ) are  $\sim 10\text{ cm}^{-1}$  higher in  $\text{KReO}_4$  spectra, relative to  $\text{NaReO}_4$  (Fig. 1). Given that both cations are coordinated to the same ligand, this spectral difference must be due to an intrinsic property of the cation. This difference may be attributed to the larger covalent radius ( $203\text{ pm}$ ), atomic volume ( $45.3\text{ cm}^3/\text{mol}$ ), or K–O bond length of K relative to Na (and Na–O). Sodium has a covalent radius of  $154\text{ pm}$  and an atomic volume of  $23.7\text{ cm}^3/\text{mol}$ , which is roughly half the atomic volume of K. Literature values of average alkali metal–oxygen bond lengths are  $2.829\text{ \AA}$ <sup>[25,29]</sup> in  $\text{KTcO}_4$  and  $2.582\text{ \AA}$  in  $\text{NaReO}_4$ .<sup>[32]</sup> If the larger atomic or covalent radii or longer bond length of K (as K–O) is responsible for the higher vibrational mode in  $\text{KReO}_4$ , then there should be fewer  $\text{K}^+$  coordinated per  $\text{ReO}_4^-$ . Fewer coordinating  $\text{K}^+$  per  $\text{ReO}_4^-$ , relative to the number of coordinating  $\text{Na}^+$  per  $\text{ReO}_4^-$ , is consistent with observations by Gafurov and Aliev<sup>[33]</sup> that ‘the number of the complexing ions becomes smaller with enlargement of the ionic radius of the cation’ in alkali metal salts. Alternatively, one could pose that the degree of covalency experienced by each  $\text{ReO}_4^-$  is higher in  $\text{NaReO}_4$  (and possibly  $\text{NaTcO}_4$ ) because there are more Na–O nearest neighbors sharing charge with the ligand. This increased covalency could shift  $\text{NaReO}_4$  modes to lower wavenumbers.<sup>[25]</sup> The antisymmetric ( $\nu_3$ ) stretch ( $B_g$ ) is approximately the same in both  $\text{ReO}_4^-$  salts ( $925\text{ cm}^{-1}$ ).

**Table 1.** Raman assignments of pure Re compounds and glasses

Mode	ReO <sub>4</sub> <sup>-</sup> (aq) <sup>[14-17]</sup>	KReO <sub>4</sub> <sup>[18-20,52,53]</sup>	KReO <sub>4</sub> (PNNL)	NaReO <sub>4</sub> <sup>[19,20,52]</sup>	NaReO <sub>4</sub> (PNNL)	4000 ppm glass (PNNL)	6145 ppm glass (no SO <sub>3</sub> ) (PNNL)	10000 ppm glass position 1 (PNNL)	10000 ppm glass position 2 (PNNL)
$\nu_1$ -sym stretch	971-972 (A <sub>1</sub> )	966-967 (A <sub>g</sub> )	969 vs	958-968	957 vs	966	965	957	967
$\nu_3$ -antisym stretch	918-920 (F <sub>2</sub> )	924-928 (B <sub>g</sub> )	926 w	924-928	924 w	925	922	924	924
$\nu_4$ -sym bend	333 (F <sub>2</sub> )	897-900 (E <sub>g</sub> )	898 m	887-888	887 m	896	896	887	898
$\nu_2$ -antisym bend	331-333 (E)	346-351 (B <sub>g</sub> )	352 w	360-372	372 w	349	348	350, 371	350
$\nu_T$ (cation) lattice	F2	334-338 (A <sub>g</sub> )	339 w	334-335	332 w	337	338	333	336
$\nu_L$ (ReO <sub>4</sub> <sup>-</sup> ) lattice	F1	326-332 (B <sub>g</sub> )	325	325	—	330	—	—	—
$\nu_T$ (ReO <sub>4</sub> <sup>-</sup> ) lattice	F2	158-160* (E <sub>g</sub> )	—	181-185*	176 vw	—	—	—	—
Unassigned		151* (B <sub>g</sub> )	—	145-156*	144 vw	106	106	108	108
		125-128* (A <sub>g</sub> )	142 vw	131-132*	—	—	—	—	—
		107-114* (E <sub>g</sub> )	108 w	84-89*	83 w	—	—	—	—
		65-73* (E <sub>g</sub> )	67 vw	77-80*	—	—	—	—	—
		55-59* (B <sub>g</sub> )	—	—	—	—	—	—	—
			1002, 762, 620, 520				93, 90	390 (artifact)	

Raw spectra can be found online in the Supporting Information. Columns denoted [Pacific Northwest National Laboratory (PNNL)] are measurements from this current work. For new crystalline measurements, the relative strength of peaks is indicated by vw (very weak), w (weak), m (medium), and vs (very strong).

\* Denoted value in range is value at 77 K<sup>[20]</sup>; lattice modes move to lower wavenumber as temperature is increased. Note that Johnson<sup>[19]</sup> and Brown<sup>[53]</sup> disagree slightly on the mode assignments for lattice modes of the alkali perhenates.

**Table 2.** Raman assignments of pure Tc compounds and glasses

Mode	TcO <sub>4</sub> <sup>-</sup> (aq) <sup>[15,16,18,22-24]</sup>	KTCO <sub>4</sub> <sup>[17,18,25]</sup>	KTCO <sub>4</sub> (PNNL)	NaTCO <sub>4</sub> (PNNL)	Surface salt	1000 ppm glass	2000 ppm glass	3000 ppm glass	4000 ppm glass	4000 ppm particle	BS glass <sup>[22]</sup>
$\nu_1$ -sym stretch	910-912 (A <sub>1</sub> )	913 (A <sub>g</sub> )	910 vs	902 vs	905 vs	911	913	904, 913	905, 912	901	915
$\nu_3$ -antisym stretch	904-908 (F <sub>2</sub> )	920 (B <sub>g</sub> )	917 m	918 w	919 m	919 m	920	920	920	916	—
$\nu_4$ -sym bend	323-325 (F <sub>2</sub> )	887 (E <sub>g</sub> )	885 s	877 s	879 s	888	888	888, 878	889, 879	877	—
$\nu_2$ -antisym bend	336 (E)	327 (B <sub>g</sub> )	327 m	322 m	326 s	328	329	324	327	323	325
$\nu_T$ (cation) lattice	F2	360 (A <sub>g</sub> )	358 w	377 w	377 w	377 w	361	377	378	377	—
$\nu_L$ (TcO <sub>4</sub> <sup>-</sup> ) lattice	F1	348-351 (B <sub>g</sub> )	347 vw	363 w	365 m	365 m	350, 360	349, 366	350, 366	364	—
$\nu_T$ (TcO <sub>4</sub> <sup>-</sup> ) lattice	F2	104	—	166 vw	162 vw	162 vw	167	167	167	162	—
Unassigned		70	138 vw	138 vw	134 w	142	140	140	140	135	—
			102 w	98 m	—	—	—	—	—	98	—
			70 vw	859	849, 126 sh	851	999, 862, 126	851	849, 129	849, 129	—

Raw spectra can be found online in the Supporting Information. Columns denoted [Pacific Northwest National Laboratory (PNNL)] are measurements from this current work. For new crystalline measurements, the relative strength of peaks is indicated by vw (very weak), w (weak), m (medium), vs (very strong), and sh(shoulder).

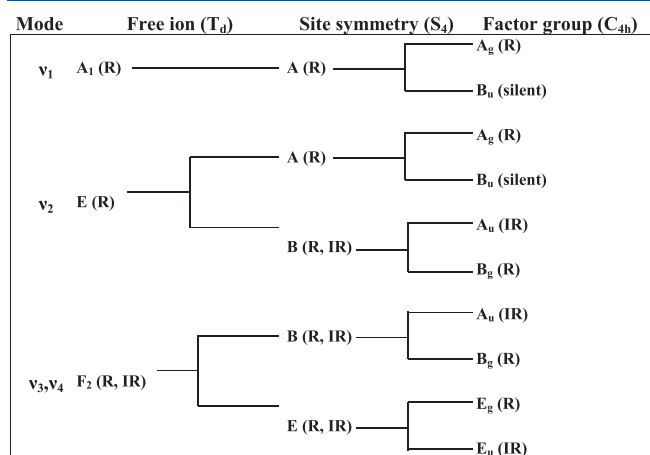


**Figure 3.** Group theory correlation diagram for  $\text{ReO}_4^-$  and  $\text{TcO}_4^-$  free-ion modes and corresponding modes in alkali perrhenate and pertechnetate salts ( $C_{4h}$  symmetry). R indicates a Raman-active mode and IR indicates an infrared-active mode.

Two well-resolved bending modes occur at 352 and 339  $\text{cm}^{-1}$  in  $\text{KReO}_4$ , with a poorly resolved shoulder at 325  $\text{cm}^{-1}$ . Similarly, two bending modes occur at 372 and 332  $\text{cm}^{-1}$  in  $\text{NaReO}_4$ . This larger energy separation (40  $\text{cm}^{-1}$ ) from  $\text{NaReO}_4$  indicates a greater difference in oscillator strengths of these bending modes relative to  $\text{KReO}_4$ . This larger difference in oscillator strengths may indicate that  $\text{Na}^+$  has two distinctly different bond lengths or bond angles amongst nearest neighbor  $\text{Na}^+$  in the crystalline lattice.

A significant difference exists between the Raman spectra of the crystalline pertechnetates and crystalline perrhenates. In the perrhenates, the symmetric stretch ( $\nu_1$ ) occurs well above the two antisymmetric stretching bands. In the pertechnetates, the symmetric stretch lies between the two antisymmetric stretching bands (Fig. 2). In this case, the role of  $\text{K}^+$  and  $\text{Na}^+$  in coordination with  $\text{ReO}_4^-$  and  $\text{TcO}_4^-$  is approximately the same, and the principal difference lies with the role of  $\text{TcO}_4^-$  in these complexes. This downward shifting of the pertechnetate salt vibrations suggests a significantly increased degree of covalency of pertechnetate in both the Na and K salts, relative to the perrhenates. Increased covalency is consistent with the shorter Tc–O bond length seen in  $\text{KTcO}_4$  (1.724 Å) versus the Re–O bond length of  $\text{KReO}_4$  (1.733 Å).<sup>[29]</sup>

In a similar trend to the perrhenates, crystalline  $\text{KTcO}_4$  exhibits  $\sim 10 \text{ cm}^{-1}$  higher stretching bands relative to  $\text{NaTcO}_4$ , with the exception of the antisymmetric ( $\nu_3$ ) stretch ( $B_g$ ) at  $\sim 917 \text{ cm}^{-1}$ . Again, it is concluded that the larger  $\text{K}^+$  maintains a more open tetrahedral structure than Na during pertechnetate stretching (Fig. 2). The pertechnetates also express three bending modes instead of two as observed in the perrhenates. Two subordinate bending modes occur with approximately a 10- $\text{cm}^{-1}$  difference between them, along with a stronger band offset to lower wavenumbers. This lower band is likely a polarized bending mode as the band intensity is much stronger than the subordinate bending modes; however, the confocal Raman spectrometer was not configurable to collect polarized spectra. Interestingly, the band separation between the subordinate bands and the stronger bend is significantly larger in  $\text{NaTcO}_4$  (42  $\text{cm}^{-1}$ ) than  $\text{KTcO}_4$  (21  $\text{cm}^{-1}$ ). Again, one could pose that this lower wavenumber band could be a symmetric bending mode with greater covalency than the antisymmetric bends.

## Glass network

Raman spectra from the borosilicate matrix of Re-containing and Tc-containing glasses exhibited two broad envelopes, one containing primarily Si–O–Si bending modes (650–250  $\text{cm}^{-1}$ )<sup>[34]</sup> and the second Si–O–Si stretching modes (1200–800  $\text{cm}^{-1}$ ).<sup>[35]</sup> Generally, the strong bands in the Si–O–Si stretching region correlate to an increasing number of bridging oxygens (BOs) per  $\text{SiO}_4$  with increasing wavenumbers. However, some variability exists in the reported frequencies of these bands. McMillan<sup>[36]</sup> described band frequencies for Na and K borosilicates as near 1100, 950–930, 900, and 850  $\text{cm}^{-1}$  with successively greater degrees of silicate polymerization with increasing wavenumber. These bands are conventionally described as  $Q^4$ ,  $Q^3$ ,  $Q^2$ ,  $Q^1$ , with 0, 1, 2, and 3 nonbridging oxygens (NBOs) per silicate unit, respectively. The 850  $\text{cm}^{-1}$  band was said to first appear at 40 mol% of alkali oxide ( $M_2O = \text{Li}_2O, \text{Na}_2O, \text{K}_2O$ ) and increased in intensity with increasing  $M_2O$  addition. The 990  $\text{cm}^{-1}$  described in the succeeding text was likely promoted from the 950–930  $\text{cm}^{-1}$  range because of the high molar percentage of silica (50%  $\text{SiO}_2$ ).<sup>[36]</sup> Parkinson *et al.*<sup>[37]</sup> identified four Si–O–Si stretches at 1150, 1065, 970, and 925  $\text{cm}^{-1}$  from  $\text{Cs}_2\text{O}$ -borosilicate glasses and correlated them to  $Q^4(B)$ ,  $Q^3$ ,  $Q^4(B)$ , and  $Q^2$ , respectively. In this nomenclature,  $Q^4(B)$  species are fully coordinated tetrahedral Si predominantly bonded to two Si and two B next nearest neighbors. The high-frequency band identified at 1150  $\text{cm}^{-1}$  occurs only as a weak shoulder in spectra and decreases in intensity with decreasing silica content.

In this study, the relative intensities of silicate stretches between 1200 and 800  $\text{cm}^{-1}$  varied between different surface sites probed by the Raman laser as exemplified by spectra from the 1000 ppm Tc glass (Fig. S1(a), Supporting Information). Three different spectra yield varying band intensities from Si–O–Si stretching at 1095 ( $Q^4$ ), 990 ( $Q^3$ ), and 920 ( $Q^2$ )  $\text{cm}^{-1}$ . These bands, attributed to Si–O–Si stretching<sup>[34]</sup> in the silicate bonding network, also have some contribution from antisymmetric and symmetric stretching of tetrahedral  $\text{TcO}_4^-$  visible at 919, 880, and 912  $\text{cm}^{-1}$  (Fig. S1(a), Supporting Information). The strength of the  $\text{TcO}_4^-$  contributions to glass spectra increased with increasing Tc additions (Fig. S1(b), Fig. S2(a, b), Supporting Information). A salt removed from the surface of the 4000 ppm Tc glass is compared with pure crystalline  $\text{NaTcO}_4$  (Fig. S3, Supporting Information). Similarly, antisymmetric and symmetric stretching from tetrahedral  $\text{ReO}_4^-$  contributed to network stretching bands.<sup>[14–17]</sup> The relatively sharp band at 990  $\text{cm}^{-1}$  appearing in the base glass and Re and Tc glasses was attributed to Si–O–Si stretching and not to symmetric stretching of  $\text{SO}_4^{2-}$ . The base glass contains only 0.16 wt.% (0.13 mol%) of  $\text{SO}_3$  and, despite the large scattering cross section of sulfur, the observed band is too strong (and too broad) to be from the trace quantity of  $\text{SO}_3$ . This band also occurs in spectra from the 6415 ppm Re glass without  $\text{SO}_3$ .

The Si–O–Si bending modes are broad and poorly resolved, showing weak peaks at  $\sim 570, 540, 490, 437,$  and  $330 \text{ cm}^{-1}$ . These modes significantly overlap and provide little useful information regarding the coordinating environments in the borosilicate matrix. Generally, these poorly resolved bands resemble silicate glasses containing high molar percentages of alkali oxides ( $M_2O$ ) with weak unresolved bands at 590, 560, and 520  $\text{cm}^{-1}$ . McMillan<sup>[36]</sup> notes that bands at 610–590 and 560–520  $\text{cm}^{-1}$  'are not simply derived from the 500 and 600  $\text{cm}^{-1}$  bands of vitreous silica, but are new bands introduced with addition of metal oxide'. At high molar additions of  $\text{Na}_2\text{O}$  (20%) to silicate glasses, Raman bands were

observed at 530, 495, and 450  $\text{cm}^{-1}$  by Furukawa and White.<sup>[27]</sup> Sharma *et al.*<sup>[35]</sup> in their analyses of  $\text{SiO}_2$  glass attributed a band at 430  $\text{cm}^{-1}$  to vibrations of six-membered rings of  $\text{SiO}_4$  and a band at 490  $\text{cm}^{-1}$  to vibrationally isolated symmetric stretching of Si–O–Si from four-membered rings of  $\text{SiO}_4$  tetrahedra.

A singular broad band exists between the stretching and bending regions discussed earlier. This weak band at 781  $\text{cm}^{-1}$  may be due to silicon vibrating against its tetrahedral oxygen cage, the silicon moving symmetrically with respect to the bridging oxygen.<sup>[36]</sup>

A weak and poorly resolved band at 770  $\text{cm}^{-1}$ , observed in glass spectra, has been attributed to vibrations of six-membered borate rings with one or two  $[\text{BO}_4]$  units.<sup>[27]</sup> Another weak and broad band  $\sim 630 \text{ cm}^{-1}$  may be due to short-range ordering by B or possibly  $\text{SiO}_3$  chain units. This band was attributed to  $\text{Na}_3\text{B}_3\text{O}_6$  from crystallized  $\text{Na}_2\text{O} \cdot 0.5 \cdot \text{SiO}_2 \cdot 0.5 \cdot \text{B}_2\text{O}_3$  glass.<sup>[27]</sup> Lastly, a weak high-frequency mode at  $\sim 1400 \text{ cm}^{-1}$  is attributed to antisymmetric stretching of trigonally coordinated boron ( $\text{BO}_3$ )<sup>-</sup> within the borosilicate lattice. Trigonal boron also has a Raman-active vibration  $\nu_4(\text{E}')$  at 545  $\text{cm}^{-1}$ , which may be contributing to the band observed at 540  $\text{cm}^{-1}$  discussed earlier.

### Rhenium in glass

The symmetric stretch ( $\nu_1$ ) of  $\text{KReO}_4$  in glass occurs at 966  $\text{cm}^{-1}$  with two antisymmetric stretches ( $\nu_3$ ) at 896 and 925  $\text{cm}^{-1}$ .<sup>[18–20]</sup> The intensity of the 896  $\text{cm}^{-1}$  band is twice that of the 925  $\text{cm}^{-1}$  band, consistent with group theory predictions ( $2 \times B_g = E_g$ ).<sup>[13]</sup> The weak bands at 349, 337, and 330  $\text{cm}^{-1}$  are attributed to bending vibrations of tetrahedrally coordinated  $\text{ReO}_4^-$ . Spectral splitting of the  $\nu_2(\text{A}_g)$  band at 331  $\text{cm}^{-1}$  was predicted to give another band at 343  $\text{cm}^{-1}$  ( $\Delta\nu=12 \text{ cm}^{-1}$ ), because of tetrahedral distortion.<sup>[12]</sup> This 343  $\text{cm}^{-1}$  degenerate bend was not observed in Re glass spectra; however, the observed bands agreed well with those of crystalline  $\text{KReO}_4$ .

Repeated spectral collection from 4000 and 6415 ppm Re glasses yielded very few spectra with evidence of  $\text{ReO}_4^-$ . Two Raman spectra from the 4000 ppm Re glass, with a derived spectrum showing  $\text{KReO}_4$  bands are shown in Fig. S4 (Supporting Information). The  $\text{KReO}_4$  spectrum derived by spectral subtraction shows bands at 966, 925, 896, 349, 337, 330, and 106  $\text{cm}^{-1}$  (Fig. S4, Supporting Information). Nearly identical  $\text{KReO}_4$  vibrations were observed from the 6415 ppm Re glass (Table 1 and Fig. S5, Supporting Information). The solubility of Re in these glasses has been shown to be 3000 ppm,<sup>[4]</sup> and the 4000 ppm glass has shown no evidence of crystallization in the bulk glass (by XRD) and no visual evidence of salt formation on the surface.<sup>[7]</sup> Unlike bulk Raman spectroscopy, which showed no evidence of crystallinity on the 4000 ppm Re glass,<sup>[7]</sup> the Raman microscopy suggested  $\text{KReO}_4$  crystals, and optical microscopy confirmed the presence of white crystals decorating cracks in the glass produced by cooling. As the glass cooled in the ampoule, thermal stresses caused it to crack, while the salt was still molten, and it was pulled into the cracks where it crystallized. However, only 1 of 16 spectra taken for this glass contained sharp peaks, suggesting that these peaks are probably due to crystalline phases.

Several Raman peaks from the 10 000 ppm Re glass are nearly identical to those from 4000 to 6415 ppm Re glasses. Spectra of the 10 000 ppm Re glass show  $\text{ReO}_4^-$  vibrations of varying intensity superimposed on broad Si–O and O–Si–O stretching between 1200 and 800  $\text{cm}^{-1}$  (Fig. S6, Supporting Information). However, the bands at 956, 924, 887, and 370  $\text{cm}^{-1}$  are consistent with  $\text{NaReO}_4$ .

It is likely that at higher added Re concentration, there is more ionic interaction of  $\text{ReO}_4^-$  with the elevated  $\text{Na}^+$  concentration (21 wt.%  $\text{Na}_2\text{O}$ ) of the glass matrix, tending to form  $\text{NaReO}_4$ . The downward shifting of  $\text{NaReO}_4$  bands, relative to  $\text{KReO}_4$  bands, is likely due to increased covalency of  $\text{Na}^+ \text{--} \text{ReO}_4^-$  bonding.<sup>[25]</sup> The 10 000 ppm Re glass has been shown to contain crystals of alkali perrhenate species of both  $\text{NaReO}_4$  and  $\text{KReO}_4$ .<sup>[4]</sup> The upper panel of Fig. 4 shows a progression of Raman spectra from crystalline  $\text{KReO}_4$  (bottom) and  $\text{NaReO}_4$  (top) and 10 000, 4000, and 10 000 ppm Re glasses (derived spectra). The 4000 and lowest 10 000 ppm Re glass spectra were the most similar to  $\text{KReO}_4$ . However, the 10 000 ppm Re glass exhibits Raman peaks of  $\text{KReO}_4$ ,  $\text{NaReO}_4$ , or both, depending on the subsampling of the glass.

### Technetium in glass

Raman spectra from Tc-containing glasses showed varying band intensities from  $\text{TcO}_4^-$ , similar to that variability previously described for the perrhenates. Low concentrations of  $\text{TcO}_4^-$  ( $\leq 1000$  ppm Tc) yielded weak peaks superimposed on the broad bands of the glass matrix (Fig. S1(a), Supporting Information). There was also significant heterogeneity in the observed spectra at different locations on the same glass surface, particularly if the surface was from the top of the melt. Above the  $\text{TcO}_4^-$  solubility limit (2000 ppm for glass as prepared and 3000 ppm for glass under slightly reducing conditions<sup>[8]</sup>), the glass surface was covered with crystalline pertechnetate salt when cooled to room temperature. Fractures formed in the glass during later stages of cooling were sometimes in-filled by still molten pertechnetate

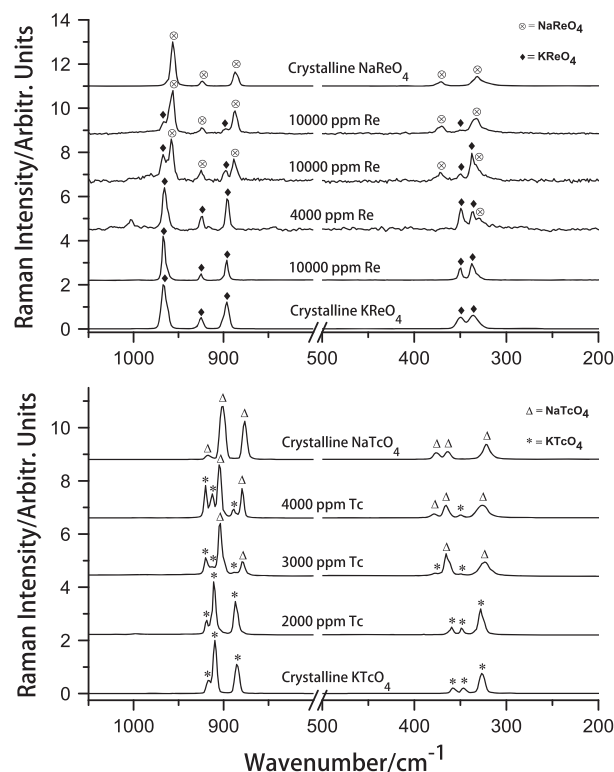


**Figure 4.** Raman spectra of perrhenate glasses and crystalline perrhenates and pertechnetate glasses and crystalline pertechnetates. Silicate features have not been removed from these spectra. Symbols indicate some characteristic peaks of the alkali perrhenate and pertechnetate phases.

salt. In some cases, pertechnetate salts collected in surface pores of the cooled glass and, in other cases, formed well-shaped crystals, suggesting vapor phase deposition. Care was taken to obtain spectra from glass surfaces visibly free of crystalline precipitates, unless of specific interest.

Generally, as Tc concentrations in glasses increased, the characteristic Raman bands of  $\text{TcO}_4^-$  stretching and bending became better resolved and allowed discrimination from the glass matrix. Spectra acquired from glasses containing 2000, 3000, and 4000 ppm Tc (Figs. S1(b), S2(a), S2(b), Supporting Information) exhibited much stronger  $\text{TcO}_4^-$  stretching and bending modes and low wavenumber external modes. These latter modes are typically associated with vibrations in crystalline lattices but are here referring to translational and rotational vibrations of the alkaline metal to oxygen bond of the  $\text{TcO}_4^-$  ion in glass.<sup>[17,18]</sup>

Notably, as Tc target concentrations increased from 2000 to 3000 to 4000 ppm in the glasses, there were gradual ingrowths of new stretching and bending bands. Figure 4 shows stacked Raman spectra of pure crystalline  $\text{KTcO}_4$  (bottom) and  $\text{NaTcO}_4$  (top) and 2000, 3000, and 4000 ppm Tc glasses (derived spectra). Trending from bottom to top in this figure, the stretching and bending vibrations of  $\text{KTcO}_4$  as the salt and then in glasses become more consistent with crystalline  $\text{NaTcO}_4$ . The spectrum of the 4000 ppm glass appears to contain both  $\text{KTcO}_4$  and  $\text{NaTcO}_4$ . Individually, indexed spectra of these salt phases are found in Fig. 2 and the glasses in Fig. S1 and Fig. S2 (Supporting Information).

Similarly to the previous discussion regarding higher perrhenate concentrations, it is likely that increasing  $\text{KTcO}_4$  concentrations in glasses makes higher  $\text{TcO}_4^-$  concentrations available for ionic interaction with very high Na concentrations (21 wt.%  $\text{Na}_2\text{O}$ ) in the glass matrix during melting. This inference necessitates at least partial equilibrium of  $\text{NaTcO}_4$  and  $\text{KTcO}_4$  in the same volume of glass excited by the laser. The process of  $\text{Na}^+$  exchanging for  $\text{K}^+$  from  $\text{KTcO}_4$  may have been controlled by the difference in melting points of  $\text{NaTcO}_4$  and  $\text{KTcO}_4$ , which Vida<sup>[38]</sup> measured using calorimetry to be 378 °C and 532 °C, respectively. This difference in melting temperature may have limited the amount of Na that exchanged for K and predisposed the formation of  $\text{KTcO}_4$  over  $\text{NaTcO}_4$  during cooling.

Alkali cations above the concentration needed to compensate network forming anions are attributed to coordinating with NBOs and becoming segregated from the network forming cations and BOs in glasses. The segregation and coalescence of these excess alkali cations and NBOs into microscopic channels have been proposed as a mechanism for enhanced movement of cations in silicate glasses.<sup>[39]</sup> The observed  $\text{Na}^+$  for  $\text{K}^+$  exchange likely occurred within these channels in proximity to  $\text{ReO}_4^-$  and  $\text{TcO}_4^-$  anions distributed within the LAW glass. It is thought that many cations such as neodymium,<sup>[40]</sup> molybdenum,<sup>[41]</sup> sulfur,<sup>[42,43]</sup> and likely rhenium<sup>[7]</sup> exist as oxyanion polyhedra along with halides<sup>[44,45]</sup> in a 'depolymerized zone' disconnected from the glass network, which at significant concentration can form 'percolation channels'.<sup>[46]</sup> The alternative to the assumption that the oxyanion (e.g. molybdate) is in a depolymerized zone<sup>[41]</sup> is that it exists as isolated tetrahedra.<sup>[47]</sup> If it is assumed that Re and Tc behave in the latter way, one would expect the Raman spectrum to consist of single bending and stretching modes, such as was observed by McKeown *et al.*<sup>[22]</sup> in their Tc-containing glasses. If, however, for kinetic or concentration reasons, the Tc (or Re) tended to cluster together in zones rich with alkali, one might expect the Raman spectra to be more characteristic of

the crystal field-splitting because of nearby alkali, as is observed in the current work.

Although the observed Na/K anion exchange provides evidence of chemical mixing in the glass, it does not prove the added  $\text{KReO}_4$  or  $\text{KTcO}_4$  salts were completely melted in the glass. Therefore, it cannot be ruled out that some sharp Raman peaks from glasses may be due to crystalline  $\text{KReO}_4$  or  $\text{KTcO}_4$  inclusions. It is unclear whether these structures were formed from the original starting materials (i.e. were not adequately homogenized), were formed during cooling (i.e. nanostructures in low concentration, not detectable by XRD or optical microscopy), or were present in disordered 'depolymerized zones' at melt temperatures but crystallized on cooling. Melting points of crystalline metasilicates ( $\text{K}_2\text{O}\cdot\text{SiO}_2$ , 976 °C;  $\text{Na}_2\text{O}\cdot\text{SiO}_2$ , 1088 °C) and disilicates ( $\text{K}_2\text{O}\cdot 2\text{SiO}_2$ , 1015 °C;  $\text{Na}_2\text{O}\cdot 2\text{SiO}_2$ , 874 °C) are significantly lower than that of crystalline  $\text{SiO}_2$  (1723 °C).<sup>[48,49]</sup> Brawer and White<sup>[50]</sup> suggest from this melting data that the Si–O networks are not 'grossly altered' when metasilicates and disilicates melt and that only the alkali–NBO bonds are broken on melting. They go on to propose that 'in passing from the crystal to the melt the Si–O network becomes disordered without significantly altering its short-range order and general topological structure'.<sup>[50]</sup> The argument for incomplete homogenization of the glass comes from observations by Ebert *et al.*<sup>[51]</sup> that glasses, similar to those considered here but containing 1500 ppm Tc as  $\text{NaTcO}_4$ , showed inclusions by scanning electron microscopy when melted at 1100 °C but not when melted at 1200 °C. Similarly, McKeown *et al.*<sup>[22]</sup> melted 1580 ppm Tc glass at 1250 °C compared with the 1000 °C used for the glasses investigated here.

## Conclusions

Spectra of perrhenate and pertechnetate glasses exhibited sharp Raman bands, characteristic of crystalline salt species, superimposed on spectral features of the borosilicate matrix. The perrhenate glasses exhibited consistent Raman stretching and bending modes at the 4000, 6415, and 10,000 ppm Re concentrations. With the exception of the 10 000 ppm Re glass, all Raman bands were consistent with crystalline  $\text{KReO}_4$ . The 10 000 ppm Re glass exhibited bands consistent with both crystalline  $\text{KReO}_4$  and crystalline  $\text{NaReO}_4$ . At this higher concentration, there exist two populations of  $\text{ReO}_4^-$ , one associated with  $\text{Na}^+$  and another associated with  $\text{K}^+$ . The weaker external modes (translational, rotational) observed in the crystalline solids were only observed in one spectrum of the 4000 ppm Re glass ( $106\text{ cm}^{-1}$ ) and a few of the 10 000 ppm Re glass spectra ( $146$  and  $108\text{ cm}^{-1}$ ).

Raman spectra of the pertechnetate glasses showed gradually increasing  $\text{TcO}_4^-$  band intensities consistent with increasing addition of  $\text{KTcO}_4$ . However, there exists a significant degree of heterogeneity in the glasses as indicated by widely varying intensities of  $\text{TcO}_4^-$  bands from individual glasses. The 1000 ppm Tc glass exhibited very weak  $\text{KTcO}_4$  bands superimposed on Si–O–Si stretching and bending vibrations. Spectra from glasses with Tc concentrations of 2000, 3000, and 4000 ppm exhibited much stronger  $\text{TcO}_4^-$  stretching and bending modes and low wavenumber external modes. Acquisition of the Raman spectrum of  $\text{NaTcO}_4$  enabled identification of Raman bands appearing in spectra of the 3000 and 4000 ppm Tc glasses as being due to formation of  $\text{NaTcO}_4$  in the presence of  $\text{KTcO}_4$ . Therefore, there are at least two populations of  $\text{TcO}_4^-$  species at higher concentrations in glass, one associated with  $\text{Na}^+$  and the other associated

with  $K^+$ . The possibility exists that another population of  $TcO_4^-$  exists in the glass that shares charges with both Na and K ions, but none were observed in the spectra. These findings are consistent with the observations by Greaves and Ngai<sup>[39]</sup> who stated 'Once the concentration of modifying oxide exceeded the percolation threshold ( $x > 0.16$ , where  $x$  is the mole fraction of modifying oxide), these micro-segregated regions would coalesce to form channels which in turn would offer energetically advantageous pathways for ionic transport.'

These results and their interpretation have strong implications for the long-term stability of Tc in nuclear waste glass formulations. Both pertechnetate and perrhenate glasses exhibit characteristic Raman bands of their precursor chemicals at intermediate concentrations in glass. Indications are that pertechnetate and perrhenate glasses contain a continuum of anionic complexes associated with  $K^+$  or  $Na^+$  concentrations in the melt, and their relative abundances are controlled by the concentrations of added  $K_2TcO_4$  or  $K_2ReO_4$ , respectively. It appears the high  $Na^+$  concentration (21 wt.%  $Na_2O$ ) in the base glass easily displaces  $K^+$  through mass action at elevated  $K_2TcO_4$  and  $K_2ReO_4$  concentrations. Indeed, Vida<sup>[38]</sup> noted that the alkali cation in the Tc salt strongly influences the degree of Tc retention in borosilicate glasses, as both  $Na_2TcO_4$  and  $K_2TcO_4$  were better retained in the glass relative to  $Cs_2TcO_4$ .

The base glass composition also has a strong effect on the equilibrium speciation of pertechnetate and perrhenate in the glass melt and consequently on long-term durability in storage. It seems likely that the sharp  $TcO_4^-$  and  $ReO_4^-$  bands are due to crystalline or nanocrystalline species, not visible under light microscopy. Resolving the identity of these species will be important for determining the ultimate durability of a Tc-containing glass waste. However, observed spectral features suggest that some stretching and bending vibrations of  $ReO_4^-$  and  $TcO_4^-$  complexes may be used as an indicator of relative bond strengths or bond lengths of Re–O and Tc–O bonds. Strongly covalent bonding of the pertechnetate anion to alkali metals in the glass suggests better long-term chemical stability of the resulting mixture. Subsequent glass formulations will need to address apparent heterogeneities in individual glasses to ensure more homogeneous mixing.

### Acknowledgements

This work was supported by the Department of Energy's Waste Treatment and Immobilization Plant Federal Project Office under the direction of Dr Albert A. Kruger. The authors thank Mary Bliss and two anonymous reviewers for the thorough comments on the manuscript. Pacific Northwest National Laboratory is operated by the Battelle Memorial Institute for the US DOE under contract DE-AC05-76RL01830. A portion of the research was performed using the Environmental Molecular Sciences Laboratory (EMSL), a national scientific user facility sponsored by the DOE's Office of Biological and Environmental Research and located at Pacific Northwest National Laboratory.

### References

- [1] J. Vienna, *Int. J. Appl. Glass Sci.* **2010**, *1*, 309.
- [2] F. Mann, Annual summary of the integrated facility performance assessment for 2004, CH2M HILL Hanford Group, Inc., Richland, WA, DOE/ORP-2000-19 Revision 4, **2004**.
- [3] B. J. Riley, J. S. McCloy, A. Goel, M. Liezers, M. J. Schweiger, J. Liu, C. P. Rodriguez, D.-S. Kim, *J. Amer. Ceram. Soc.* **2013**, *96*, 1150.
- [4] J. S. McCloy, B. J. Riley, A. Goel, M. Liezers, M. J. Schweiger, C. P. Rodriguez, P. Hrma, D.-S. Kim, W. W. Lukens, A. A. Kruger, *Environ. Sci. Technol.* **2012**, *46*, 12616.
- [5] W. W. Lukens, D. A. McKeown, A. C. Buechele, I. S. Muller, D. K. Shuh, I. L. Pegg, *Chem. Mater.* **2007**, *19*, 559.
- [6] J. G. Darab, P. A. Smith, *Chem. Mater.* **1996**, *8*, 1004.
- [7] A. Goel, J. S. McCloy, C. F. Windisch, B. J. Riley, M. J. Schweiger, C. P. Rodriguez, J. M. F. Ferreira, *Int. J. Appl. Glass Sci.* **2013**, *4*, 42.
- [8] C. Z. Soderquist, M. J. Schweiger, D. S. Kim, W. W. Lukens, J. S. McCloy, *J. Nucl. Mater.*, accepted.
- [9] K. I. Petrov, A. F. Kuzina, N. I. Dolgorukova, Y. M. Golovin, V. I. Spitsyn, *Dokl. Akad. Nauk SSSR* **1972**, *206*, 909.
- [10] J. Beintema, *Z. Krist.* **1937**, *97*, 300.
- [11] R. Fonteyne, *Natuurwetenschappelijk* **1938**, *20*, 20.
- [12] H. H. Claassen, A. J. Zielen, *J. Chem. Phys.* **1954**, *22*, 707.
- [13] D. F. Heath, J. W. Linnett, *Trans. Faraday Soc.* **1948**, *44*, 878.
- [14] K. I. Petrov, V. G. Pervykh, M. B. Varfolomeev, V. E. Plyushchev, *J. Appl. Spectrosc.* **1968**, *8*, 401.
- [15] N. Weinstock, H. Schulze, *J. Chem. Phys.* **1973**, *59*, 5063.
- [16] H. H. Eysel, B. Kanellakopulos, *J. Raman Spectrosc.* **1993**, *24*, 119.
- [17] A. Müller, W. Rittner, *Spectrochim. Acta A* **1967**, *23*, 1831.
- [18] R. H. Busey, O. L. Keller, Jr., *J. Chem. Phys.* **1964**, *41*, 215.
- [19] R. A. Johnson, M. T. Rogers, G. E. Leroi, *J. Chem. Phys.* **1972**, *56*, 789.
- [20] J. Korppi-Tommola, V. Devarajan, R. J. C. Brown, H. F. Shurvell, *J. Raman Spectrosc.* **1978**, *7*, 96.
- [21] A. Tougeri, S. Cristol, E. Berrier, V. Briois, C. La Fontaine, F. Villain, Y. Joly, *Phys. Rev. B* **2012**, *85*, 125136.
- [22] D. A. McKeown, A. C. Buechele, W. W. Lukens, D. K. Shuh, I. L. Pegg, *Radiochim. Acta* **2007**, *95*, 275.
- [23] L. J. Basile, J. R. Ferraro, P. LaBonville, M. C. Wall, *Coord. Chem. Rev.* **1973**, *11*, 21.
- [24] M. V. Mikelsons, T. C. Pinkerton, *Appl. Radiat. Isot.* **1987**, *38*, 569.
- [25] M. J. Sarsfield, A. D. Sutton, F. R. Livens, I. May, R. J. Taylor, *Acta Crystallogr. C* **2003**, *59*, i45.
- [26] J. McCloy, B. J. Riley, A. Goel, M. Liezers, M. J. Schweiger, C. P. Rodriguez, C. Windisch, P. Hrma, D. S. Kim, J. Liu, W. W. Lukens, A. A. Kruger, Rhenium solubility in borosilicate nuclear waste glass: implications for the processing and immobilization of technetium-99, Pacific Northwest National Laboratory, Richland, WA, PNNL-21553, Rev 0, **2012**.
- [27] T. Furukawa, W. White, *J. Mater. Sci.* **1981**, *16*, 2689.
- [28] J. C. Morrow, *Acta Crystallogr.* **1960**, *13*, 443.
- [29] B. Krebs, K.-D. Hasse, *Acta Crystallogr. B* **1976**, *32*, 1334.
- [30] K. Schwochau, *Z. Naturforsch.* **1962**, *17a*, 630.
- [31] M. Baluka, J. Hanuka, Jezowska-Trzebiatowska, *B. Acad. Pol. Sci.-Chim.* **1972**, *20*, 271.
- [32] A. Atzesdorfer, K. J. Range, *Z. Naturforsch. B* **1995**, *50*, 1417.
- [33] M. M. Gafurov, A. R. Aliev, *Spectrochim. Acta A* **2004**, *60*, 1549.
- [34] S. K. Sharma, J. F. Mammone, M. F. Nicol, *Nature* **1981**, *292*, 140.
- [35] S. K. Sharma, T. F. Cooney, Z. Wang, S. van der Laan, *J. Raman Spectrosc.* **1997**, *28*, 697.
- [36] P. McMillan, *J. Raman Spectrosc.* **1984**, *69*, 622.
- [37] B. G. Parkinson, D. Holland, M. E. Smith, C. Larson, J. Doerr, M. Affatigato, S. A. Feller, A. P. Howes, C. R. Scales, *J. Non-Cryst. Solids* **2008**, *354*, 1936.
- [38] J. Vida, The chemical behavior of technetium during treatment of high-level radioactive waste [translated from German by JR Jewett], Battelle Pacific Northwest Laboratory, Richland, WA, PNL-TR-497, **1994**.
- [39] G. N. Greaves, K. L. Ngai, *J. Non-Cryst. Solids* **1994**, *172–174*, Part 2, 1378.
- [40] D. Caurant, P. Loiseau, O. Majerus, V. Aubin-Chevaldonnet, I. Bardez, A. Quintas, *Glasses, Glass-Ceramics and Ceramics for Immobilization of Highly Radioactive Nuclear Wastes*. Nova Science Publishers, Inc., New York, **2009**.
- [41] D. Caurant, O. Majerus, E. Fadel, A. Quintas, C. Gervais, T. Charpentier, D. Neuville, *J. Nucl. Mater.* **2010**, *396*, 94.
- [42] L. Backnaes, J. Deubener, *Rev. Miner. Geochem.* **2011**, *73*, 143.
- [43] D. A. McKeown, I. S. Muller, H. Gan, I. L. Pegg, C. A. Kendziora, *J. Non-Cryst. Solids* **2001**, *288*, 191.
- [44] F. A. Lifanov, M. I. Ojovan, S. V. Stefanovsky, R. Burcel. Feasibility and experience to vitrify NPP operational waste. In *WM'03*. February 23–27, 2003, Tucson, AZ, **2003**.

- [45] D. A. McKeown, H. Gan, I. L. Pegg, W. C. Stolte, I. N. Demchenko, *J. Nucl. Mater.* **2011**, *408*, 236.
- [46] G. N. Greaves, *J. Non-Cryst. Solids* **1985**, *71*, 203.
- [47] G. Calas, M. Le Grand, L. Galois, D. Ghaleb, *J. Nucl. Mater.* **2003**, *322*, 15.
- [48] W. A. Weyl, E. C. Marboe, *The Constitution of Glasses*, Vol. I, Interscience, New York, **1961**.
- [49] W. A. Weyl, E. C. Marboe, *The Constitution of Glasses*, Vol. II, Interscience, New York, **1964**.
- [50] S. A. Brawer, W. B. White, **1975**, *63*, 2421.
- [51] W. L. Ebert, A. J. Bakel, D. L. Bowers, E. C. Buck, J. W. Emery, *Ceram. Trans.* **1998**, *87* (*Environmental Issues and Waste Management Technologies in the Ceramic and Nuclear Industries III*), 431.
- [52] Kohlrausch, 'Perrheniumsäure.' 396 (1972 reprint Heyden & Son Ltd). In *Ramanspektren*. Akademische Verlagsgesellschaft Becker & Erler Kom.-Ges., Leipzig, **1943**.
- [53] R. J. C. Brown, R. M. Lynden-Bell, I. R. McDonald, M. T. Dove, *J. Phys. Condens. Matter* **1994**, *6*, 9895.

## Supporting information

Additional supporting information may be found in the online version of this article at the publisher's web site.